NeuroImage xxx (2010) xxx–xxx

Contents lists available at ScienceDirect

NeuroImage

journal homepage: www.elsevier.com/locate/ynimg

Technical Note

Striatal functional connectivity networks are modulated by fMRI resting state conditions

Kaundinya Gopinath [a,b,c,*], Wendy Ringe [d], Aman Goyal [c], Kirstine Carter [d], Hubert R. Dinse [e], Robert Haley [b], Richard Briggs [a,b,c]

[a] Department of Radiology, University of Texas Southwestern Medical Center, Dallas, TX 75390, USA
[b] Department of Internal Medicine, University of Texas Southwestern Medical Center, Dallas, TX 75390, USA
[c] Graduate Program in Biomedical Engineering, University of Texas Southwestern Medical Center, Dallas, TX 75390, USA
[d] Department of Psychiatry, University of Texas Southwestern Medical Center, Dallas, TX 75390, USA
[e] Institut für Neuroinformatik, Neural Plasticity Lab, Ruhr-University, Bochum, Germany

ARTICLE INFO

Article history:
Received 27 February 2010
Revised 6 July 2010
Accepted 8 July 2010
Available online xxxx

Keywords:
fcMRI
Functional connectivity
Striatum
Fronto-striatal networks
Resting state conditions
BOLD

ABSTRACT

Resting state fluctuations in blood oxygenation level dependent functional connectivity magnetic resonance imaging (BOLD fcMRI) time-series have been increasingly employed to study functional connectivity networks in healthy and diseased brain. FcMRI studies have been conducted under a number of different conditions, including resting eyes open, visual fixation and finger tapping. BOLD fcMRI networks are believed to reflect both anatomically constrained spontaneous fluctuations and state-dependent activity. In this study, state-dependence of functional connectivity to dorsal and ventral striatum was assessed with fcMRI during an eyes open resting state condition (REST) and during continuous 3 Hz transcutaneous electrical nerve stimulation (TENS), with the a priori hypotheses: (1) dorsal striatum connectivity with sensorimotor/attention networks will be stronger during TENS compared to REST, (2) ventral striatum connectivity with limbic system emotion-processing network will be weaker during TENS compared to REST and (3) ventral striatum connectivity with sensorimotor/attention networks will be stronger during TENS compared to REST. These hypotheses were confirmed by the results obtained, indicating that resting state BOLD fMRI networks reflect, in substantial measure, state-dependent activity.

Introduction

Coherent resting state fluctuations in blood oxygenation level dependent (BOLD) functional magnetic resonance imaging (fMRI) data in functionally connected regions of the brain were first observed more than a decade ago (Biswal et al., 1995). Resting state fluctuations in BOLD fMRI time-series have been increasingly employed to study functional connectivity networks in healthy brain and in disease (Buckner et al., 2008; Fox and Raichle, 2007; Greicius, 2008; Williamson, 2007). Functional connectivity MRI (fcMRI) studies have been conducted under a number of different conditions: resting eyes open (Fox et al., 2005; Van Dijk et al., 2010; Yan et al., 2009), eyes closed (Fox et al., 2005; Greicius et al., 2009; Van Dijk et al., 2010; Yan et al., 2009), visual fixation (Buckner et al., 2009; Fox et al., 2005; Van Dijk et al., 2010; Yan et al., 2009), focal visual stimulation (Bianciardi et al., 2009a), viewing pictures with positive, negative or neutral valences (Anand et al., 2005), finger tapping (Morgan and Price, 2004), continuous performance tasks (Amann et al., 2009), tactile stimulation (Mantini et al., 2009) and acupuncture (Hui et al., 2009). A number of recent studies have explicitly studied the state dependence of different functional connectivity networks (Bianciardi et al., 2009a; Fransson, 2006; Hampson et al., 2002; Newton et al., 2007; Van Dijk et al., 2010; Yan et al., 2009).

BOLD fcMRI networks are believed to reflect both anatomically constrained spontaneous fluctuations and state-dependent activity (Buckner et al., 2009; Fox and Raichle, 2007). The intent of this study was to examine how functional connectivity in specific well-established brain networks is modulated by resting state condition. Classical studies (Drevets and Raichle, 1998; Price et al., 1996) reveal a reciprocal relationship between cognitive and emotion systems in the brain. The activation in dorsal and lateral aspects of the prefrontal cortex and the dorsal anterior cingulate increases during attention-demanding tasks compared to emotional tasks. Also, activation in these same areas decreases when an emotional component is added to the task. At the same time, activation in limbic areas involved in emotion processing, (such as ventral prefrontal cortex and ventral anterior cingulate) increases in emotion compared to attention-only tasks, and decreases during attention-demanding tasks. Attention and

* Corresponding author. Department of Radiology, Division of Neuroradiology, UT Southwestern Medical Center, 5323 Harry Hines Boulevard, Dallas, TX 75390-8896, USA. Fax: +1 214 648 3904.
E-mail address: kaundinya.gopinath@utsouthwestern.edu (K. Gopinath).

1053-8119/$ – see front matter © 2010 Elsevier Inc. All rights reserved.
doi:10.1016/j.neuroimage.2010.07.021

sensorimotor networks often show concomitant patterns of activation during sensory and attention tasks (Drevets and Raichle, 1998; Fan et al., 2005; Kim et al., 2006; Wenderoth et al., 2005a, b) and are often not distinguished from each other in animal literature (Haber et al., 1995; Neafsey, 1990; Ongur et al., 1998; Ongur and Price, 2000). In this study, we examined whether differences in sensory and attention demands of resting state conditions lead to analogous changes in functional connectivity in sensorimotor/attention networks and in emotion-processing networks.

The striatum receives projections from the entire cerebral cortex (Alexander et al., 1986, 1990; Lawrence et al., 2000; Postuma and Dagher, 2006) and has rich connections to both sensorimotor/attention and limbic emotion-processing networks. Hence it can serve as an optimal seed region to assess reciprocal changes in functional connectivity in these two systems. The striatum can be divided into ventral striatum (VS) and dorsal striatum (DS), which are thought to be highly inter-connected regions with a dissociation of functions (Haber, 2003; Price et al., 1996; Voorn et al., 2004). The most superior aspect of the DS is strongly associated with sensorimotor experiences (Haber, 2003; Packard and Knowlton, 2002; White and McDonald, 2002) and more inferior aspects of the DS are associated with higher order cognitive functions such as attention (Voorn et al., 2004). VS is strongly connected to the limbic emotion processing system comprised of areas such as the amygdala, ventral anterior cingulate, ventromedial and ventrolateral prefrontal cortex, medial dorsal nucleus of the thalamus and hippocampus (Drevets and Raichle, 1998; Heidbreder and Groenewegen, 2003; Morgane et al., 2005; Price et al., 1996). Intra-striatal connections are asymmetric, with significantly more VS efferents to DS and sensorimotor and attention networks than DS efferents to VS and the limbic system (Joel and Wiener, 2000). VS acts as an interface between emotion processing and sensorimotor/attention systems (Haber et al., 1995; Ongur et al., 2003) and can be recruited in sensorimotor paradigms.

Transcutaneous electrical nerve stimulation (TENS) has been shown to activate areas that are part of sensorimotor and/or attention networks, including primary and secondary somatosensory cortex, insula, premotor and motor cortex, supplementary motor area (SMA), dorsal anterior cingulate, dorsolateral prefrontal cortex, paracentral lobule, parietal lobe, thalamus, basal ganglia and cerebellum (Arienzo et al., 2006; Ferretti et al., 2007; Fors et al., 1996; Huang et al., 2010; Pleger et al., 2003; Porro et al., 2004). TENS can also be controlled by the experimenter without being confounded by subject task performance (e.g. as in finger-tapping). Thus TENS provides a convenient and controllable way to stimulate these networks. In this study, changes in striatal functional connectivity networks were examined during an eyes open resting (REST) condition compared to a continuous transcutaneous electrical median nerve stimulation that was not painful. The a priori hypotheses in this study were: (1) the DS connectivity to sensorimotor/attention areas involved in median nerve stimulation will be higher during TENS compared to REST, (2) the VS connectivity to limbic system emotion processing areas will be higher during REST compared to TENS and (3) the VS connectivity to sensorimotor/attention areas involved in median nerve stimulation will be higher during TENS compared to REST. Confirmation of the a priori hypotheses would add evidence to the notion that resting state BOLD fMRI networks reflect, in substantial measure, state-dependent activity.

Methods

Subjects

Thirteen healthy subjects (5 F, 8 M, mean age 32 years, all right-handed, mean education 17 years) participated. Written informed consent was obtained for all subjects.

Task description

Each subject performed fcMRI scans under the following three resting state conditions.

(1) Resting eyes open with transcutaneous median nerve stimulation: For the TENS condition, the subjects were asked to lie motionless in the scanner with their eyes open. Continuous transcutaneous electrical median nerve stimulation that was not painful was applied to the index fingers of both hands with a custom-built device (Pleger et al., 2003). The frequency of stimulation was set to 3 Hz and the intensity of the stimulation was adjusted to 1.15 times the sensory threshold (defined as the intensity where subjects could feel minimal stimulation with certainty). The subjects were instructed to focus on the sensation of electrical stimulation on the fingers resulting in a slight increase in attention and sensory task demands.
(2) Resting eyes open with visual fixation (VISFIX): The subjects were instructed to lie motionless and fixate on an image with a red cross on a gray background which was projected on a screen placed behind the magnet bore and viewed with a back-projection mirror affixed to the head coil. After the scan, subjects were asked if they were able to fixate on the cross for the duration of the scan. Results of the VISFIX condition are not presented in this paper.
(3) Resting Eyes Open (REST): This provided an unstructured and self-regulated neutral affective condition. For the REST fcMRI scans the subjects were asked to lie motionless in the scanner with their eyes open. Subjects were asked to blink at a normal rate and were asked after the end of the run if they kept their eyes open throughout the scan.

Each resting state condition was acquired once. The scan duration for each of the three conditions above was 10 min and 58 s The order

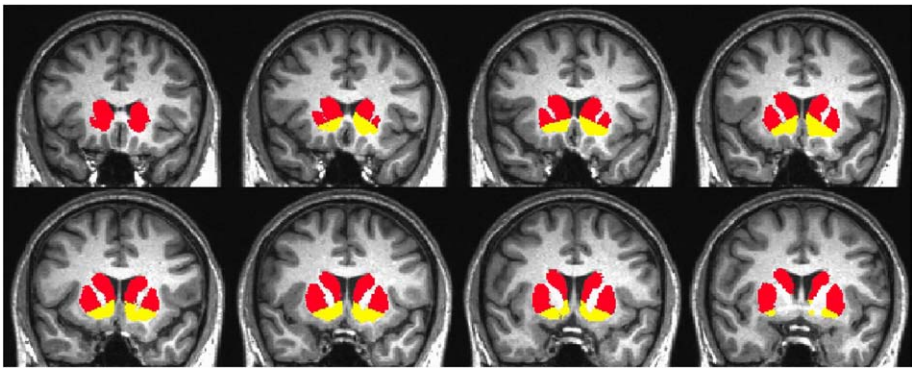

Fig. 1. Bilateral dorsal (red) and ventral (yellow) striatum tracings on a representative subject. (For interpretation of the references to colour in this figure legend, the reader is referred to the web version of this article.)

Please cite this article as: Gopinath, K., et al., Striatal functional connectivity networks are modulated by fMRI resting state conditions, NeuroImage (2010), doi:10.1016/j.neuroimage.2010.07.021

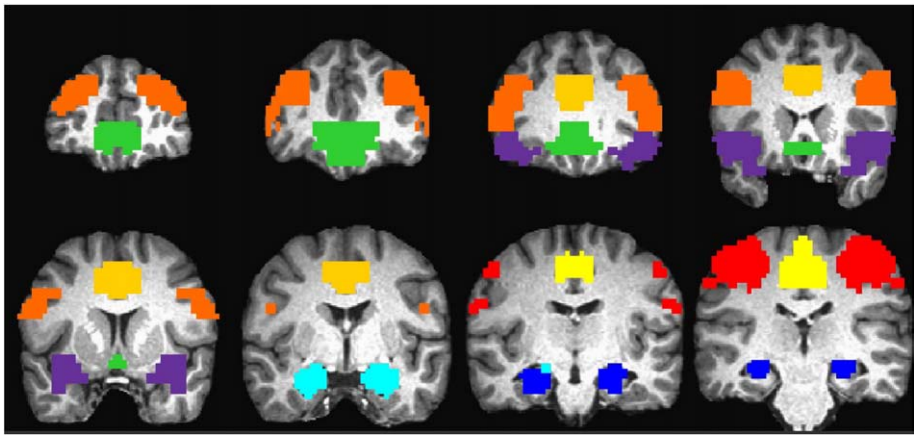

Fig. 2. A priori ROIs used for connectivity analysis: left and right primary somatosensory cortex (red); left and right dorsolateral prefrontal cortex (orange); bilateral paracentral lobule (yellow); bilateral dorsal anterior cingulate (orange-yellow); left and right amygdala (cyan); left and right hippocampus (blue); bilateral ventral anterior cingulate (green); left and right ventrolateral prefrontal cortex (purple). Left hemisphere is on the right side of the figure. Coronal slices are at Talairach co-ordinate locations 53A to 24P in steps of 11 mm. (For interpretation of the references to colour in this figure legend, the reader is referred to the web version of this article.)

of the runs was same for all subjects, TENS followed by VISFIX and then REST.

Image acquisition

Resting state BOLD fMRI images were acquired on a 3 T Siemens Trio TIM scanner with a 12-channel receiver array head coil and an EPI sequence using the following parameters: FOV = 220 mm; TR/TE = 2000/28 ms; flip angle (FA) = 90°; 74 × 74 matrix size; 37 interleaved axial slices (no slice gap); 326 scan volumes; acquisition time = 10 min and 58 s. The slice thickness was adjusted according to brain size to keep the relative volume averaging similar across subjects. Five subjects each required 3.4 mm and 3.5 mm slices, respectively, to cover the whole brain, and one subject was scanned with 3 mm slices. The slightly decreased SNR expected in the data of the subject scanned with 3 mm slices is mitigated by the proportionately larger number of voxels aggregated during spatial smoothing, and thus no subject-specific correction for SNR was performed. Prospective real-time motion correction (Thesen et al., 2000) implemented by Siemens as the 3D-PACE option was employed with all EPI fMRI scans to minimize motion artifacts. A time-of-flight MR angiogram (TR/TE/FA = 26 ms/6 ms/40°; 0.9 mm × 0.9 mm in-plane resolution) with the same FOV and slice prescriptions as the EPI fMRI scans was acquired for angiographic reference. A whole-brain 3D T1-weighted MPRAGE sequence (FOV = 230 mm; TR/TI/TE/FA = 2250 ms/900 ms/3 ms/9°; 0.9 mm × 0.9 mm × 1 mm resolution) was acquired to provide anatomic detail. All scans were acquired with GRAPPA parallel imaging, acceleration factor = 2 with 24 (36 for MPRAGE) phase encode reference lines. Foam padding was provided to minimize head motion. Biopac (Goleta, CA) respiration belt and finger pulse oximeter were provided to acquire physiological waveforms time-locked to fMRI acquisition. The sampling rate for the physiological responses was set to 200 Hz. The temporal sequences of individual heart beats were extracted from the Biopac finger pulse oximeter waveform with supervised application of Matlab's *findpeaks* program. The output of the program was inspected manually (and the input parameters adjusted adaptively as needed) to ensure all the heart beats were encoded in the form of a cardiac pulse spike train vector.

Data analysis

Data from one subject was discarded due to malfunction of the physiological response monitoring equipment. Another subject had an abnormally large sinus cavity that resulted in susceptibility artifacts impacting signal from the ventral striatum. For the remaining 11 subjects, data analysis was performed with AFNI (Cox, 1996) and FSL (Smith et al., 2004) software and in-house programs written in Matlab (Natick, MA). The first three volumes of the fcMRI time-series were removed to ensure attainment of magnetization steady state. The voxel time-series were then detrended of signal related to cardiac and respiratory oscillations at their respective main frequencies and

Table 1
Locations of a priori regions of interest.

A priori regions of interest in Talairach template co-ordinates	Left–right extent	Anterior–posterior extent	Superior–inferior extent	ROI volume (μl)
Emotion-processing Network ROIs				
Ventral Anterior Cingulate	18 L–18 R	3 A–55 A	11 I–6 S	23328
L Ventrolateral Prefrontal Cortex	17 L–55 L	8 A–38 A	21 I–3 S	14904
R Ventrolateral Prefrontal Cortex	17 R–55 R	8 A–38 A	21 I–3 S	14904
L Amygdala	14 L–30 L	4 A–10 P	10 I–24 I	4347
R Amygdala	14 R–30 R	4 A–10 P	10 I–24 I	4347
L Hippocampus	13 L–31 L	2 P–38 P	24 I–2 S	9126
R Hippocampus	13 R–31 R	2 P–38 P	24 I–2 S	9126
Sensory/attention network ROIs				
Dorsal Anterior Cingulate	14 L–14 R	0 A–32 A	20 S–50 S	17037
L Dorsolateral Prefrontal Cortex	17 L–55 L	4 A–55 A	9 S–41 S	27648
R Dorsolateral Prefrontal Cortex	17 R–55 R	4 A–55 A	9 S–41 S	27648
Paracentral Lobule	18 L–18 R	12 P–43 P	43 S–64 S	21060
L Somatosensory Cortex	19 L–64 L	13 P–41 P	31 S–69 S	18576
R Somatosensory Cortex	19 R–64 R	13 P–41 P	31 S–69 S	18576

Please cite this article as: Gopinath, K., et al., Striatal functional connectivity networks are modulated by fMRI resting state conditions, NeuroImage (2010), doi:10.1016/j.neuroimage.2010.07.021

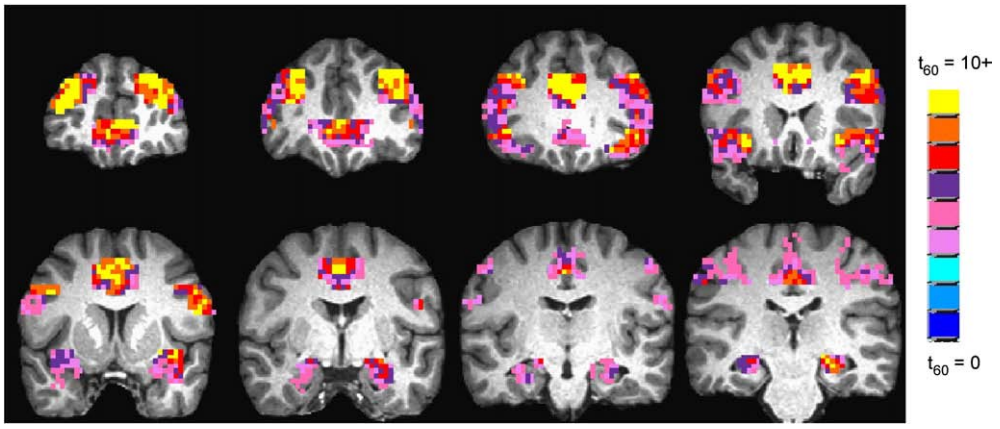

Fig. 3. Combined REST condition dorsal striatum functional connectivity maps (ANOVA treatment-mean *t*-scores) from 13 a priori ROIs ($p<0.0001$), overlaid on high-resolution T1-weighted images of a representative subject. Left hemisphere is on the right side of the figure. Coronal slices are at Talairach co-ordinate locations 53A to 24P in steps of 11 mm.

first harmonics using RETROICOR (Glover et al., 2000). The resulting voxel-time series were temporally shifted to account for differences in slice acquisition times. The 3D scan volumes of the physiological-noise-corrected, time-shifted fcMRI dataset were registered to the last volume of the time-series (the volume closest in time to the T1-weighted high resolution anatomic scan) with a rigid, intensity-based, iterative, linearized, weighted least squares algorithm (Cox and Jesmanowicz, 1999) and spatially smoothed with an isotropic Gaussian filter (FWHM = 5 mm). Low-frequency fluctuations in BOLD signal arising from changes in heart rate (in mean beats per minute; MBPM) and respiration volume per time (RVT) were attenuated using techniques based on existing literature (Bianciardi et al., 2009b; Birn et al., 2006; Shmueli et al., 2007) . For each resting state run, a RVT regressor was generated from the Biopac respiration trace by first dividing the difference between maximum and minimum respiration belt positions by the time between consecutive maxima (Birn et al., 2006); and then interpolating the resultant RVT vector to a 2 s^{-1} sampling rate. A heart-rate trace was generated by expressing the time difference between consecutive cardiac peaks (in the pulse-oximeter waveform) in beats per minute. The MBPM (mean beats per minute) regressor was generated from the heart-rate trace by averaging the heart rate within a 6-s window centered around each TR (Chang et al., 2009). Voxel time series were detrended of signal proportional to 31 lagged realizations of the RVT regressor (lag times = −30 s to +30 s in steps of 2 s) and 7 lagged realizations of the MBPM regressor (lag times = −12 s to +12 s in steps of 2 s) in a single regression step. The resultant time-series were detrended of signal proportional to motion parameters estimated by the image-registration algorithm and then low-pass filtered (Chebyshev II filter; cutoff frequency = 0.12 Hz) to better isolate low frequency resting state BOLD functional connectivity fluctuations.

Striatum ROIs

FSL's sub-cortical segmentation program *FIRST* was employed to segment the sub-cortical structures that comprise the bilateral striatum: caudate, putamen and nucleus accumbens. The high resolution T1-weighted anatomic image and the overlays of the sub-cortical structures were rotated so that the anterior (AC) and posterior (PC) commissures lay on the same transaxial plane. DS and VS regions of interest (ROIs) were then parcellated for both hemispheres through an established procedure described in a recent paper (Mawlawi et al., 2001). As described in this paper, the boundary between the VS and DS on the AC-PC aligned anatomic image was defined by a line joining (a) the intersection between the outer edge of the putamen with a vertical line going through the most superior and lateral point of the internal capsule; and (b) the center of the portion of the AC transaxial plane overlying the striatum. This line was extended to the internal edge of the caudate until it reached the lateral ventricle. This line demarcating the boundary of DS and VS was drawn on all coronal slices beginning caudally at the level of the anterior commissure and ending rostrally at the disappearance of the head of the caudate. These tracings were resampled and overlaid on each subject's fcMRI image data. Voxels sensitive to corruption by susceptibility artifact and those at brain edges were excluded from analysis by means of a brain masking program available in the AFNI software, and voxels in the striatum partially occupied by white matter or ventricles were also

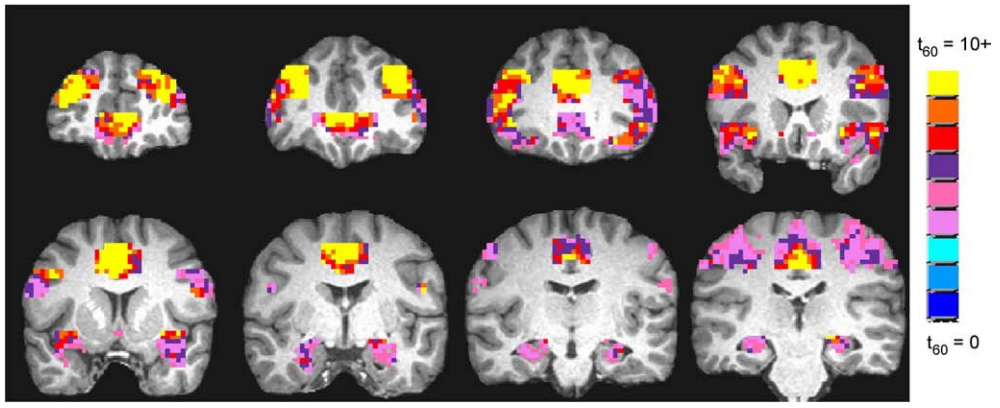

Fig. 4. Combined TENS condition dorsal striatum functional connectivity maps (ANOVA treatment-mean *t*-scores) from 13 a priori ROIs ($p<0.0001$), overlaid on high- resolution T1-weighted images of a representative subject. Left hemisphere is on the right side of the figure. Coronal slices are at Talairach co-ordinate locations 53A to 24P in steps of 11 mm.

Please cite this article as: Gopinath, K., et al., Striatal functional connectivity networks are modulated by fMRI resting state conditions, NeuroImage (2010), doi:10.1016/j.neuroimage.2010.07.021

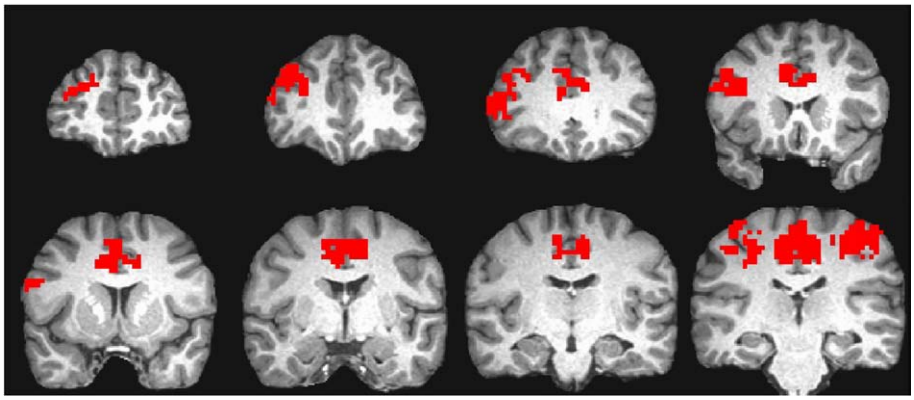

Fig. 5. Combined TENS vs. REST dorsal striatum functional connectivity difference maps from 6 a priori sensory/attention network ROIs, overlaid on high-resolution T1-weighted images of a representative subject. Significant ($p<0.0002$) TENS > REST clusters are in red. Left hemisphere is on the right side of the figure. Coronal slices are Talairach co-ordinate locations 53A to 24P in steps of 11 mm. (For interpretation of the references to colour in this figure legend, the reader is referred to the web version of this article.)

masked out. Further, voxels in the DS (VS) mask occupied more than 20% by VS (DS) were also masked out. Fig. 1 shows the dorsal and ventral striatum tracings in AC-PC space from a representative subject. The registrations between the T1-weighted anatomic scan and the fcMRI scans were visually examined using anatomic landmarks (e.g. edges of ventricles) and found to be within 1–2 voxels. Co-registration of EPI datasets to the T1-weighted anatomic scan (using affine transformation modules in FSL/AFNI) did not yield visually appreciable improvements in the registration of the EPI-to-T1-weighted anatomic scan. Hence, the first-level connectivity analysis was performed without coregistration to avoid errors arising from resampling and interpolation related to coregistration.

Connectivity analysis

Left and right hemisphere DS and VS ROI-averaged time-series were obtained and served as reference vectors for cross-correlation analysis, performed under a linear regression framework. Each subject's high resolution anatomic image was spatially normalized to the AFNI Talairach template. The resultant transformation matrix was used to warp to standard space, for subsequent group analysis, the maps of least squares estimates of the linear regression proportionality coefficients ("fit coefficients") of each voxel's time-series with the left and right DS and VS ROI-averaged reference vectors. Connectivity maps for the dorsal and ventral striatum were obtained with two-factor analyses of variance (ANOVA: Laterality × Condition) on the spatially normalized fit coefficients. Functional connectivity of the dorsal and ventral striatum during each of the conditions was assessed with treatment-mean *t*-tests. Differences in functional connectivity (of both DS and VS) between different states were assessed with between-conditions *t*-contrasts. The group *t*-statistic maps were clustered and cluster-level significances, controlled for multiple comparisons, were obtained from Monte Carlo simulation of the process of image generation, spatial correlation of voxels, intensity thresholding, masking and cluster identification (Forman et al., 1995) through the *AlphaSim* program in AFNI. Each a priori ROI used for hypothesis testing (see below) was used as a separate mask and clusters within these masks were obtained for each of the ANOVA *t*-contrast comparisons between conditions and the ANOVA treatment-mean *t*-tests within each condition. Cluster-level significance was then obtained by applying the *AlphaSim* program to data in each mask. Finally, Bonferroni correction was employed (as described below) to control for multiple comparisons (independent and exclusive ROI masks) used for testing of a given hypothesis.

ROI analyses rationale

To test the a priori hypotheses, several a priori ROIs were created within the two networks (sensorimotor/attention and limbic emotion processing). Six a priori ROIs were created to examine sensorimotor/attention networks. Left and right primary somatosensory cortices (S1) were chosen because of their rich connections to the dorsal striatum (Haber and Calzavara, 2009; Price et al., 1996; Voorn et al., 2004) and the substantial sensory component in the TENS condition (Ferretti et al., 2007; Pleger et al., 2003; Porro et al., 2004). Paracentral lobule was selected since it is activated in a number of median nerve stimulation experiments (Fors et al., 1996; Huang et al., 2010). Dorsal anterior cingulate (DACC) and left and right dorsolateral prefrontal cortices (DLPFC) were chosen for their well-known involvement in both attention and sensory tasks, and due to their well-documented connections to dorsal striatum (Arienzo et al., 2006; Bush et al., 2000; Drevets and Raichle, 1998; Porro et al., 2004; Pourtois et al., 2010).

Seven a priori ROIs were created in the limbic emotion-processing network. Ventral anterior cingulate (VACC), left and right ventrolateral prefrontal cortices (VLPFC), left and right amygdalae and left and right hippocampi were chosen, given both their connections with the ventral striatum and their well-documented role in emotion processing (Bengtsson et al., 2009; Bush et al., 2000; Drevets and Raichle, 1998; Manna et al., 2010; Mayberg et al., 1997).

ROI anatomical description

All a priori ROIs were created with the aid of the Talairach daemon (Lancaster et al., 2000) implemented in AFNI. An S1 ROI in each hemisphere was designated as including all of Brodmann areas (BA) 1,

Table 2
Dorsal striatum connectivity differences between TENS and REST condition in 6 a priori sensory/attention network ROIs. Voxel contrast *p*-threshold, $p<0.15$.

Sensory/Attention Network ROIs TENS > REST	Talairach maxima	Contrast cluster extent (μl)	ROI fraction occupied by cluster	Contrast cluster *p*-value
Dorsal Anterior Cingulate	4 R, 25 A, 26 S	13716	81%	0.0001
L Dorsolateral Prefrontal Cortex	NS	NS	NS	NS
R Dorsolateral Prefrontal Cortex	40 R, 17 A, 29 S	13392	49%	0.0001
Paracentral Lobule	6 L, 21 P, 47 S	13419	64%	0.0001
L Somatosensory Cortex	47 L, 27 P, 55 S	7641	41%	0.0002
R Somatosensory Cortex	28 R, 20 P, 38 S	5049	27%	0.0001

Please cite this article as: Gopinath, K., et al., Striatal functional connectivity networks are modulated by fMRI resting state conditions, NeuroImage (2010), doi:10.1016/j.neuroimage.2010.07.021

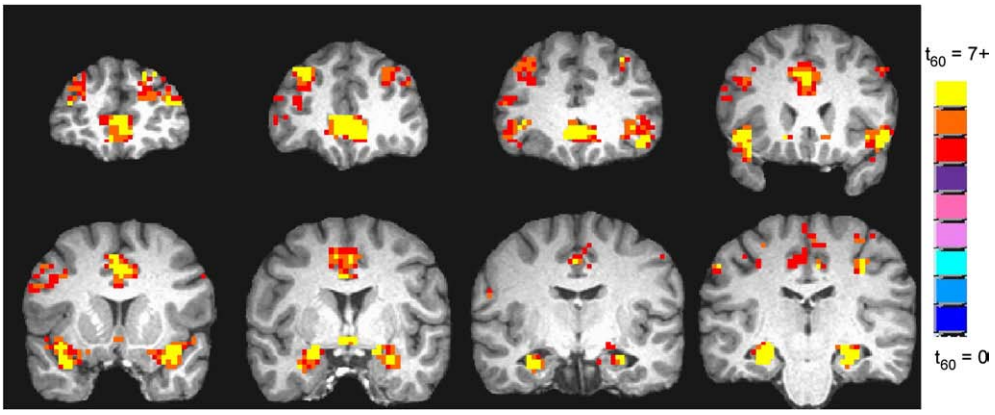

Fig. 6. Combined REST condition ventral striatum functional connectivity maps (ANOVA treatment-mean *t*-scores) from 13 a priori ROIs ($p<0.0001$), overlaid on high- resolution T1-weighted images of a representative subject. Left hemisphere is on the right side of the figure. Coronal slices are Talairach co-ordinate locations 56A to 21P in steps of 11 mm.

2 and 3 (Geyer et al., 1999; Ruben et al., 2001). All the voxels in the bilateral paracentral lobule (as labeled in the Talairach daemon) were included into an ROI. A DLPFC ROI in each hemisphere was formed by incorporating BA 46 and the lateral portion of BA 9 (Cho and Strafella, 2009; Cullen et al., 2006). Dorsal and ventral anterior cingulate were defined as the portions of BA 24 and BA 32 superior and inferior, respectively, to the genu of the corpus callosum (Bush et al., 2000). To avoid overlap with S1 and paracentral lobule, the dorsal anterior cingulate ROI extended posteriorly only to the level of anterior commissure. VLPFC ROIs in each hemisphere were comprised of the lateral aspects of BA47, as previously described (Bengtsson et al., 2009).

All ROIs were resampled to match the dimensions $(3\text{ mm})^3$ of the group ANOVA *t*-score maps. The ROIs were extended into the cortex by one voxel (3 mm) on all sides to correct for potential spatial normalization errors. Fig. 2 shows the selected ROIs and Table 1 lists the spatial extent of the ROIs. Each a priori ROI was used as a separate mask and clusters within these masks were obtained for each of the ANOVA *t*-contrast comparisons between conditions and the ANOVA treatment-mean *t*-tests within each condition. Cluster-level significance was then obtained by applying the *AlphaSim* program to data in each ROI mask. Finally, to obtain overall hypotheses-level significance, Bonferroni correction was applied by multiplying the cluster-level *p*-values by the number of exclusive and independent ROIs involved in a given hypothesis: 6 for a priori Hypothesis 1 and Hypothesis 3, 7 for Hypothesis 2 and 13 for the exploratory hypotheses involving all investigated areas. The unqualified *p*-values for functional connectivity data reported in the next section have been corrected for multiple comparisons within each ROI (using AlphaSim) and across all ROIs involved in the relevant hypotheses (Bonferroni correction).

Results and Discussion

All subjects were able to keep their eyes open for the duration of all fcMRI runs as ascertained by exit interviews. The maximal displacement calculated from estimated motion parameters was within one voxel in all the runs for all subjects. The MBPM power spectra from all subjects were similar to those obtained by other groups (Shmueli et al., 2007), with the spectral power of heart rate variability concentrated at low frequencies (below 0.03 Hz). The individual subject RVT power spectra were also consistent with others reported previously (Birn et al., 2006), with significant spectral power remaining up to 0.08 Hz. There was no significant difference between the fcMRI conditions (*t*-test $p>0.1$) in the RVT and MBPM power spectra at all sampled frequencies. The summed power (binned at 0.011 Hz bandwidth intervals) at all frequency bands also yielded no significant differences between conditions ($p>0.1$).

There were no significant laterality effects in the connectivity maps for DS and VS in any of the conditions ($p>0.4$) in any of the ROIs examined. Hence, the connectivities of the two seeds were examined after collapsing across both left and right hemisphere data. Figs. 3 and 4 show the dorsal striatum connectivity maps (treatment-mean *t*-tests) for the REST and TENS conditions, respectively, in all 13 ROIs examined in this study. Both conditions exhibited significant ($p<0.0001$) DS connectivity with voxels in all ROIs examined, although DS exhibited stronger connectivity with voxels in

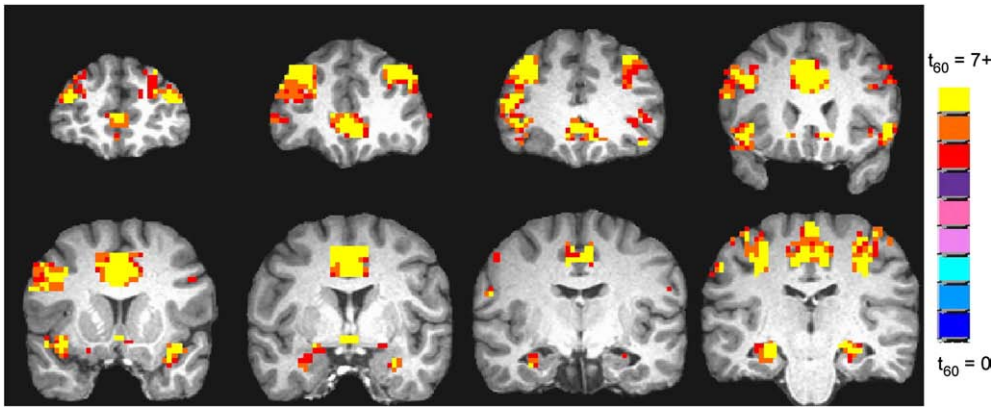

Fig. 7. Combined TENS condition ventral striatum functional connectivity maps (ANOVA treatment-mean *t*-scores) from 13 a priori ROIs (overall $p<0.0001$), overlaid on high-resolution T1-weighted images of a representative subject. Left hemisphere is on the right side of the figure. Coronal slices are Talairach co-ordinate locations 56A to 21P in steps of 11 mm.

Please cite this article as: Gopinath, K., et al., Striatal functional connectivity networks are modulated by fMRI resting state conditions, NeuroImage (2010), doi:10.1016/j.neuroimage.2010.07.021

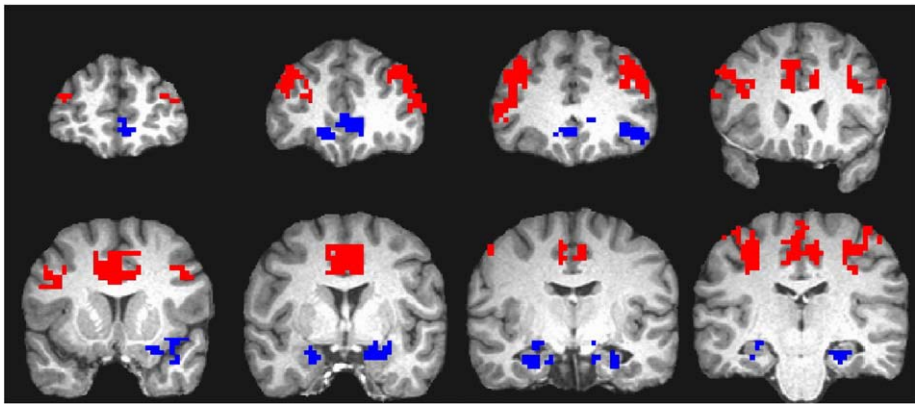

Fig. 8. Combined TENS vs REST ventral striatum functional connectivity difference maps from 6 a priori sensory and attention network ROIs and 7 a priori emotion-processing network ROIs, overlaid on high-resolution T1-weighted images of a representative subject. Significant TENS>REST ($p<0.001$) clusters are in red and REST>TENS ($p<0.04$) clusters are in blue. Left hemisphere is on the right side of the figure. Coronal slices are at Talairach co-ordinate locations; 56A to 21P in steps of 11 mm. (For interpretation of the references to color in this figure legend, the reader is referred to the Web version of this article.)

sensorimotor/attention network ROIs than those in limbic emotion-processing network ROIs for both conditions. Fig. 5 and Table 2 show the DS functional connectivity differences between the REST and TENS conditions. Consistent with a priori Hypothesis 1, DS exhibited significantly higher ($p<0.0002$) connectivity during TENS than REST in the following sensorimotor/attention ROIs: left and right S1, bilateral DACC, paracentral lobule and right DLPFC. Figs. 6 and 7 show the ventral striatum connectivity maps (treatment-mean *t*-tests) for the REST and TENS conditions, respectively, in all 13 ROIs examined in this study. Both conditions exhibited significant ($p<0.0001$) VS connectivity with voxels in the limbic emotion-processing network ROIs as well as in the ROIs in sensorimotor/attention networks examined. During the REST condition, VS exhibited stronger connectivity with voxels in the emotion-processing network ROIs than with those in sensorimotor/attention network ROIs, whereas in the TENS condition VS connectivity was similar or higher with the sensorimotor/attention network than with the emotion-processing network. Fig. 8 and Table 3 show VS functional connectivity differences between the REST and TENS conditions. Consistent with Hypothesis 2, VS connectivity was significantly higher ($p<0.04$) during REST than TENS with voxels in the emotion-processing network (blue overlays in Fig. 8), including bilateral amygdala, hippocampus and VACC, and left VLPFC. Further, VS connectivity with sensorimotor/attention areas (red overlays in Fig. 8) were significantly higher ($p<0.0001$) during TENS than REST, which is consistent with a priori Hypothesis 3. Finally, as an exploratory exercise, DS connectivity differences between TENS and REST were examined in all 7 emotion processing ROIs and no significant differences were found.

Left DLPFC failed to exhibit the hypothesized stronger DS connectivity during TENS compared to REST, and right VLPFC failed to exhibit the hypothesized weaker VS connectivity during TENS compared to REST. These could reflect the low detection power for state-dependent connectivity differences yielded by the small effect size and the relatively small sample size of 11 subjects. Also the effect sizes of connectivity differences between REST and TENS conditions were too small to reveal significant clusters in a whole brain exploratory analysis without a priori hypotheses. A statistical power analysis conducted with effect sizes for contrasts between different conditions from the present study indicates that a more comprehensive study utilizing more than 40 subjects will be needed to obtain significant DS and VS connectivity differences between the conditions at the whole-brain level with no a priori hypotheses.

The results show that DS connectivity to sensorimotor/attention areas increases with increasing sensory and attention demands (between REST and TENS). At the same time, VS connectivity to emotion processing areas decreases with increasing sensory and attention demands. This is consistent with reciprocal modulations of sensorimotor/attention and limbic emotion network activation that have been observed in previous studies (Drevets and Raichle, 1998; Price et al., 1996). VS connectivity to sensorimotor/attention areas also increases with increasing sensory and attention demands. This is

Table 3
Ventral striatum connectivity differences between TENS and REST conditions in 7 a priori emotion-processing network ROIs and 6 sensory/attention network ROIs. Voxel contrast p-threshold, $p<0.15$.

	Talairach maxima	Contrast cluster extent (μl)	ROI fraction occupied by cluster	Contrast cluster *p*-value
Emotion-processing network ROIs REST>TENS				
Ventral anterior cingulate	9 L, 46 A, 2 S	4887	21%	0.04
L ventrolateral prefrontal cortex	39 L, 17 A, 7 I	3591	25%	0.006
R ventrolateral prefrontal cortex	NS	NS	NS	NS
L amygdala	23 L, 5 P, 18I	2133	50%	0.0007
R amygdala	19 R 5 P, 10 I	1701	39%	0.01
L hippocampus	22 L, 26 P, 16 I	3132	34%	0.001
R hippocampus	38 R, 26 P, 8 I	2754	30%	0.007
Sensory/attention network ROIs TENS>REST				
Dorsal anterior cingulate	2 R, 2 A, 46 S	15147	89%	0.0001
L dorsolateral prefrontal cortex	35 L, 28 A, 26 S	6723	24%	0.001
R dorsolateral prefrontal cortex	53 R, 29 A, 11 S	11502	42%	0.0001
Paracentral lobule	11 R, 29 P, 52 S	10854	52%	0.0001
L somatosensory cortex	47 L, 28 P, 61 S	6291	34%	0.0001
R somatosensory cortex	43 R, 26P, 44 S	4941	27%	0.0004

Please cite this article as: Gopinath, K., et al., Striatal functional connectivity networks are modulated by fMRI resting state conditions, NeuroImage (2010), doi:10.1016/j.neuroimage.2010.07.021

consistent with the classic neuroanatomic literature suggesting that the VS acts as an interface between emotion processing and sensorimotor/cognition systems (Haber et al., 1995; Ongur et al., 2003) and hence could be recruited in sensory tasks such as TENS. The results also support the notion that BOLD fMRI connectivity maps reflect (at least in some measure) state-dependent activity. The most striking manifestation of this dependence is seen in the VS connectivity changes between REST and TENS (Fig. 8 and Table 3) that reveal an attenuation in functional connectivity along the limbic emotion-processing network at the same time as an enhancement in functional connectivity along sensorimotor/attention networks. State-dependence in functional connectivity networks is important, since the cognitive and emotional states of subjects (normal or diseased) during passive conditions such as REST are not well-determined. Further, data from resting state studies could be affected by the subjects' prior mood, mental state or immediate experiences (Albert et al., 2009; Miall and Robertson, 2006; Stevens et al., 2010; Waites et al., 2005), which may lead to increased variability in resting state fcMRI networks obtained from different subjects. The results also suggest the need for future studies examining the effects of increasing emotional task demands of resting state conditions on striatal connectivity maps.

Conclusion

This study confirms the hypothesis of a reciprocal relationship between the functional connectivity of the striatum within sensorimotor/attention networks, on the one hand, and emotion-processing network on the other. During TENS, there were increases in the strength of connections between the dorsal striatum and sensorimotor/attention networks, together with a concomitant decrease in the strength of the connectivity of the ventral striatum to the limbic emotion-processing network. The results add to existing evidence from prior literature that suggests that resting state fcMRI networks reflect in a large part state-dependent activity. The results also suggest that interactions between the resting state condition chosen and the regions/networks of interest for the investigation are important factors to be considered while designing fcMRI paradigms.

Acknowledgments

This study was supported by DoD grant no. DAMD 17-01-1-0741 from the U.S. Army Medical Research and Materiel Command and by VA IDIQ contract number VA549-P-0027 awarded and administered by the Dallas, TX VA Medical Center. The content of this paper does not necessarily reflect the position or the policy of the U.S. government, and no official endorsement should be inferred. Construction of the TENS stimulation device was supported by the University of Texas Southwestern Medical Center Mobility Foundation, through a grant to Dr Delaina Walker-Batson, Texas Woman's University and Dr Mark Johnson, UT Southwestern Medical Center. The authors also acknowledge Dr Jeffrey Spence and Dr Unal Sakoglu of UT Southwestern Medical Center for useful discussions and the Department of Radiology for administrative support. HRD acknowledges funding by the Bernstein Focus "State dependencies of learning" 01GQ0974.

References

Albert, N.B., Robertson, E.M., Miall, R.C., 2009. The resting human brain and motor learning. Curr. Biol. 19, 1023–1027.
Alexander, G.E., Crutcher, M.D., DeLong, M.R., 1990. Basal ganglia-thalamocortical circuits: parallel substrates for motor, oculomotor, "prefrontal" and "limbic" functions. Prog. Brain Res. 85, 119–146.
Alexander, G.E., DeLong, M.R., Strick, P.L., 1986. Parallel organization of functionally segregated circuits linking basal ganglia and cortex. Annu. Rev. Neurosci. 9, 357–381.
Amann, M., Hirsch, J.G., Gass, A., 2009. A serial functional connectivity MRI study in healthy individuals assessing the variability of connectivity measures: reduced interhemispheric connectivity in the motor network during continuous performance. Magn. Reson. Imaging.
Anand, A., Li, Y., Wang, Y., Wu, J., Gao, S., Bukhari, L., et al., 2005. Antidepressant effect on connectivity of the mood-regulating circuit: an FMRI study. Neuropsychopharmacology 30, 1334–1344.
Arienzo, D., Babiloni, C., Ferretti, A., Caulo, M., del Gratta, C., Tartaro, A., et al., 2006. Somatotopy of anterior cingulate cortex (ACC) and supplementary motor area (SMA) for electric stimulation of the median and tibial nerves: an fMRI study. Neuroimage 33, 700–705.
Bengtsson, S.L., Lau, H.C., Passingham, R.E., 2009. Motivation to do well enhances responses to errors and self-monitoring. Cereb. Cortex 19, 797–804.
Bianciardi, M., Fukunaga, M., van Gelderen, P., Horovitz, S.G., de Zwart, J.A., Duyn, J.H., 2009a. Modulation of spontaneous fMRI activity in human visual cortex by behavioral state. Neuroimage 45, 160–168.
Bianciardi, M., Fukunaga, M., van Gelderen, P., Horovitz, S.G., Shmueli, K., de Zwart, J.A., et al., 2009b. Sources of functional magnetic resonance imaging signal fluctuations in the human brain at rest: a 7T study. Magn. Reson. Imaging 27, 1019–1029.
Birn, R.M., Diamond, J.B., Smith, M.A., Bandettini, P.A., 2006. Separating respiratory-variation-related fluctuations from neuronal-activity-related fluctuations in fMRI. Neuroimage 31, 1536–1548.
Biswal, B., Yetkin, F.Z., Haughton, V.M., Hyde, J.S., 1995. Functional connectivity in the motor cortex of resting human brain using echo-planar MRI. Magn. Reson. Med. 34, 537–541.
Buckner, R.L., Andrews-Hanna, J.R., Schacter, D.L., 2008. The brain's default network: anatomy, function, and relevance to disease. Ann. NY Acad. Sci. 1124, 1–38.
Buckner, R.L., Sepulcre, J., Talukdar, T., Krienen, F.M., Liu, H., Hedden, T., et al., 2009. Cortical hubs revealed by intrinsic functional connectivity: mapping, assessment of stability, and relation to Alzheimer's disease. J. Neurosci. 29, 1860–1873.
Bush, G., Luu, P., Posner, M.I., 2000. Cognitive and emotional influences in anterior cingulate cortex. Trends Cogn. Sci. 4, 215–222.
Chang, C., Cunningham, J.P., Glover, G.H., 2009. Influence of heart rate on the BOLD signal: the cardiac response function. Neuroimage 44, 857–869.
Cho, S.S., Strafella, A.P., 2009. rTMS of the left dorsolateral prefrontal cortex modulates dopamine release in the ipsilateral anterior cingulate cortex and orbitofrontal cortex. PLoS ONE 4, e6725.
Cox, R.W., 1996. AFNI: software for analysis and visualization of functional magnetic resonance neuroimages. Comput. Biomed. Res. 29, 162–173.
Cox, R.W., Jesmanowicz, A., 1999. Real-time 3D image registration for functional MRI. Magn. Reson. Med. 42, 1014–1018.
Cullen, T.J., Walker, M.A., Eastwood, S.L., Esiri, M.M., Harrison, P.J., Crow, T.J., 2006. Anomalies of asymmetry of pyramidal cell density and structure in dorsolateral prefrontal cortex in schizophrenia. Br. J. Psychiatry 188, 26–31.
Drevets, W.C., Raichle, M.E., 1998. Reciprocal suppression of regional cerebral blood flow during emotional versus higher cognitive processes: implications for interactions between emotion and cognition. Cognit. Emotion 12, 352–385.
Fan, J., McCandliss, B.D., Fossella, J., Flombaum, J.I., Posner, M.I., 2005. The activation of attentional networks. Neuroimage 26, 471–479.
Ferretti, A., Babiloni, C., Arienzo, D., del Gratta, C., Rossini, P.M., Tartaro, A., et al., 2007. Cortical brain responses during passive nonpainful median nerve stimulation at low frequencies (0.5–4 Hz): an fMRI study. Hum. Brain Mapp. 28, 645–653.
Forman, S.D., Cohen, J.D., Fitzgerald, M., Eddy, W.F., Mintun, M.A., Noll, D.C., 1995. Improved assessment of significant activation in functional magnetic resonance imaging (fMRI): use of a cluster-size threshold. Magn. Reson. Med. 33, 636–647.
Fors, N., Merlet, I., Vanni, S., Hamalainen, M., Mauguiere, F., Hari, R., 1996. Activation of human mesial cortex during somatosensory target detection task. Brain Res. 734, 229–235.
Fox, M.D., Raichle, M.E., 2007. Spontaneous fluctuations in brain activity observed with functional magnetic resonance imaging. Nat. Rev. Neurosci. 8, 700–711.
Fox, M.D., Snyder, A.Z., Vincent, J.L., Corbetta, M., Van Essen, D.C., Raichle, M.E., 2005. The human brain is intrinsically organized into dynamic, anticorrelated functional networks. Proc. Natl Acad. Sci. USA 102, 9673–9678.
Fransson, P., 2006. How default is the default mode of brain function? Further evidence from intrinsic BOLD signal fluctuations. Neuropsychologia 44, 2836–2845.
Geyer, S., Schleicher, A., Zilles, K., 1999. Areas 3a, 3b, and 1 of human primary somatosensory cortex. Neuroimage 10, 63–83.
Glover, G.H., Li, T.Q., Ress, D., 2000. Image-based method for retrospective correction of physiological motion effects in fMRI: RETROICOR. Magn. Reson. Med. 44, 162–167.
Greicius, M., 2008. Resting-state functional connectivity in neuropsychiatric disorders. Curr. Opin. Neurol. 21, 424–430.
Greicius, M.D., Supekar, K., Menon, V., Dougherty, R.F., 2009. Resting-state functional connectivity reflects structural connectivity in the default mode network. Cereb. Cortex 19, 72–78.
Haber, S.N., 2003. The primate basal ganglia: parallel and integrative networks. J. Chem. Neuroanat. 26, 317–330.
Haber, S.N., Calzavara, R., 2009. The cortico-basal ganglia integrative network: the role of the thalamus. Brain Res. Bull. 78, 69–74.
Haber, S.N., Kunishio, K., Mizobuchi, M., Lynd-Balta, E., 1995. The orbital and medial prefrontal circuit through the primate basal ganglia. J. Neurosci. 15, 4851–4867.
Hampson, M., Peterson, B.S., Skudlarski, P., Gatenby, J.C., Gore, J.C., 2002. Detection of functional connectivity using temporal correlations in MR images. Hum. Brain Mapp. 15, 247–262.
Heidbreder, C.A., Groenewegen, H.J., 2003. The medial prefrontal cortex in the rat: evidence for a dorso-ventral distinction based upon functional and anatomical characteristics. Neurosci. Biobehav. Rev. 27, 555–579.

Please cite this article as: Gopinath, K., et al., Striatal functional connectivity networks are modulated by fMRI resting state conditions, NeuroImage (2010), doi:10.1016/j.neuroimage.2010.07.021

Huang, M.X., Lee, R.R., Gaa, K.M., Song, T., Harrington, D.L., Loh, C., et al., 2010. Somatosensory system deficits in schizophrenia revealed by MEG during a Median-Nerve Oddball Task. Brain Topogr. 23, 82–104.
Hui, K.K., Marina, O., Claunch, J.D., Nixon, E.E., Fang, J., Liu, J., et al., 2009. Acupuncture mobilizes the brain's default mode and its anti-correlated network in healthy subjects. Brain Res. 1287, 84–103.
Joel, D., Wiener, I., 2000. The connections of the dopaminergic system with the striatum in rats and primates: an analysis with respect to the functional and compartmental organization of the striatum. Neuroscience 96, 451–474.
Kim, J., Whyte, J., Wang, J., Rao, H., Tang, K.Z., Detre, J.A., 2006. Continuous ASL perfusion fMRI investigation of higher cognition: quantification of tonic CBF changes during sustained attention and working memory tasks. Neuroimage 31, 376–385.
Lancaster, J.L., Woldorff, M.G., Parsons, L.M., Liotti, M., Freitas, C.S., Rainey, L., et al., 2000. Automated Talairach atlas labels for functional brain mapping. Hum. Brain Mapp. 10, 120–131.
Lawrence, A.D., Watkins, L.H., Sahakian, B.J., Hodges, J.R., Robbins, T.W., 2000. Visual object and visuospatial cognition in Huntington's disease: implications for information processing in corticostriatal circuits. Brain 123 (Pt 7), 1349–1364.
Manna, A., Raffone, A., Perrucci, M.G., Nardo, D., Ferretti, A., Tartaro, A., et al., 2010. Neural correlates of focused attention and cognitive monitoring in meditation. Brain Res. Bull. 82, 46–56.
Mantini, D., Caulo, M., Ferretti, A., Romani, G.L., Tartaro, A., 2009. Noxious somatosensory stimulation affects the default mode of brain function: evidence from functional MR imaging. Radiology 253, 797–804.
Mawlawi, O., Martinez, D., Slifstein, M., Broft, A., Chatterjee, R., Hwang, D.R., et al., 2001. Imaging human mesolimbic dopamine transmission with positron emission tomography: I. Accuracy and precision of D(2) receptor parameter measurements in ventral striatum. J. Cereb. Blood Flow Metab. 21, 1034–1057.
Mayberg, H.S., Brannan, S.K., Mahurin, R.K., Jerabek, P.A., Brickman, J.S., Tekell, J.L., et al., 1997. Cingulate function in depression: a potential predictor of treatment response. NeuroReport 8, 1057–1061.
Miall, R.C., Robertson, E.M., 2006. Functional imaging: is the resting brain resting? Curr. Biol. 16, R998–R1000.
Morgan, V.L., Price, R.R., 2004. The effect of sensorimotor activation on functional connectivity mapping with MRI. Magn. Reson. Imaging 22, 1069–1075.
Morgane, P.J., Galler, J.R., Mokler, D.J., 2005. A review of systems and networks of the limbic forebrain/limbic midbrain. Prog. Neurobiol. 75, 143–160.
Neafsey, E.J., 1990. Prefrontal cortical control of the autonomic nervous system: anatomical and physiological observations. Prog. Brain Res. 85, 147–165 discussion 165-146..
Newton, A.T., Morgan, V.L., Gore, J.C., 2007. Task demand modulation of steady-state functional connectivity to primary motor cortex. Hum. Brain Mapp. 28, 663–672.
Ongur, D., An, X., Price, J.L., 1998. Prefrontal cortical projections to the hypothalamus in macaque monkeys. J. Comp. Neurol. 401, 480–505.
Ongur, D., Ferry, A.T., Price, J.L., 2003. Architectonic subdivision of the human orbital and medial prefrontal cortex. J. Comp. Neurol. 460, 425–449.
Ongur, D., Price, J.L., 2000. The organization of networks within the orbital and medial prefrontal cortex of rats, monkeys and humans. Cereb. Cortex 10, 206–219.
Packard, M.G., Knowlton, B.J., 2002. Learning and memory functions of the basal ganglia. Annu. Rev. Neurosci. 25, 563–593.
Pleger, B., Foerster, A.F., Ragert, P., Dinse, H.R., Schwenkreis, P., Malin, J.P., et al., 2003. Functional imaging of perceptual learning in human primary and secondary somatosensory cortex. Neuron 40, 643–653.
Porro, C.A., Lui, F., Facchin, P., Maieron, M., Baraldi, P., 2004. Percept-related activity in the human somatosensory system: functional magnetic resonance imaging studies. Magn. Reson. Imaging 22, 1539–1548.
Postuma, R.B., Dagher, A., 2006. Basal ganglia functional connectivity based on a meta-analysis of 126 positron emission tomography and functional magnetic resonance imaging publications. Cereb. Cortex 16, 1508–1521.
Pourtois, G., Vocat, R., N'Diaye, K., Spinelli, L., Seeck, M., Vuilleumier, P., 2010. Errors recruit both cognitive and emotional monitoring systems: simultaneous intracranial recordings in the dorsal anterior cingulate gyrus and amygdala combined with fMRI. Neuropsychologia 48, 1144–1159.
Price, J.L., Carmichael, S.T., Drevets, W.C., 1996. Networks related to the orbital and medial prefrontal cortex; a substrate for emotional behavior? Prog. Brain Res. 107, 523–536.
Ruben, J., Schwiemann, J., Deuchert, M., Meyer, R., Krause, T., Curio, G., et al., 2001. Somatotopic organization of human secondary somatosensory cortex. Cereb. Cortex 11, 463–473.
Shmueli, K., van Gelderen, P., de Zwart, J.A., Horovitz, S.G., Fukunaga, M., Jansma, J.M., et al., 2007. Low-frequency fluctuations in the cardiac rate as a source of variance in the resting-state fMRI BOLD signal. Neuroimage 38, 306–320.
Smith, S.M., Jenkinson, M., Woolrich, M.W., Beckmann, C.F., Behrens, T.E., Johansen-Berg, H., et al., 2004. Advances in functional and structural MR image analysis and implementation as FSL. Neuroimage 23 (Suppl 1), S208–S219.
Stevens, W.D., Buckner, R.L., Schacter, D.L., 2010. Correlated low-frequency BOLD fluctuations in the resting human brain are modulated by recent experience in category-preferential visual regions. Cereb. Cortex 8, 1997–2006.
Thesen, S., Heid, O., Mueller, E., Schad, L.R., 2000. Prospective acquisition correction for head motion with image-based tracking for real-time fMRI. Magn. Reson. Med. 44, 457–465.
Van Dijk, K.R., Hedden, T., Venkataraman, A., Evans, K.C., Lazar, S.W., Buckner, R.L., 2010. Intrinsic functional connectivity as a tool for human connectomics: theory, properties, and optimization. J. Neurophysiol. 103, 297–321.
Voorn, P., Vanderschuren, L.J., Groenewegen, H.J., Robbins, T.W., Pennartz, C.M., 2004. Putting a spin on the dorsal–ventral divide of the striatum. Trends Neurosci. 27, 468–474.
Waites, A.B., Stanislavsky, A., Abbott, D.F., Jackson, G.D., 2005. Effect of prior cognitive state on resting state networks measured with functional connectivity. Hum. Brain Mapp. 24, 59–68.
Wenderoth, N., Debaere, F., Sunaert, S., Swinnen, S.P., 2005a. The role of anterior cingulate cortex and precuneus in the coordination of motor behaviour. Eur. J. Neurosci. 22, 235–246.
Wenderoth, N., Debaere, F., Sunaert, S., Swinnen, S.P., 2005b. Spatial interference during bimanual coordination: differential brain networks associated with control of movement amplitude and direction. Hum. Brain Mapp. 26, 286–300.
White, N.M., McDonald, R.J., 2002. Multiple parallel memory systems in the brain of the rat. Neurobiol. Learn. Mem. 77, 125–184.
Williamson, P., 2007. Are anticorrelated networks in the brain relevant to schizophrenia? Schizophr. Bull. 33, 994–1003.
Yan, C., Liu, D., He, Y., Zou, Q., Zhu, C., Zuo, X., et al., 2009. Spontaneous brain activity in the default mode network is sensitive to different resting-state conditions with limited cognitive load. PLoS ONE 4, e5743.

Please cite this article as: Gopinath, K., et al., Striatal functional connectivity networks are modulated by fMRI resting state conditions, NeuroImage (2010), doi:10.1016/j.neuroimage.2010.07.021